

Analysis of Aerodynamic Load of LSU-03 (LAPAN Surveillance UAV-03) Propeller

Awang Rahmadi Nuranto¹⁾Ahmad Jamaludin Fitroh²⁾and Hendri Syamsudin³⁾

¹⁾ Student, Faculty of Mechanical and Aerospace Engineering, Institut Teknologi Bandung, Indonesia
Aeronautics Technology Center, National Institute of Aeronautics and Space (LAPAN), Indonesia

²⁾ Rocket Technology Center, National Institute of Aeronautics and Space (LAPAN), Indonesia

³⁾ Faculty of Mechanical and Aerospace Engineering, Institut Teknologi Bandung, Indonesia

Abstract. The existing propeller of the LSU-03 aircraft is made of wood. To improve structural strength and obtain better mechanical properties, the propeller will be redesigned using composite materials. It is necessary to simulate and analyze the design load. This research paper explains the simulation and analysis of aerodynamic load prior to structural design phase of composite propeller. Aerodynamic load calculations are performed using both the Blade Element Theory (BET) and the Computational Fluid Dynamic (CFD) simulation. The result of both methods show a close agreement, the different thrust forces is only 1.2 and 4.1% for two type mesh. Thus the distribution of aerodynamic loads along the surface of the propeller blades of the 3-D CFD simulation results are considered valid and ready to design the composite structure. The CFD results is directly imported to the structure model using the Direct Import CFD / One-Way Fluid Structure Interaction (FSI) method. Design load of propeller is chosen at the flight condition at speed of 20 m/s at 7000 rpm.

1. Introduction

Propeller is component of several types of aircraft to be local components for aircraft produced in Indonesia.

Various types of aircraft ranging from passenger aircraft and Unmanned Aerial Vehicle (UAV), turbopropeller engine to piston requires a propeller as a force-changer of rotational motion into a thrust force by utilizing the aerodynamic forces acting on the propeller. The design of the propeller is essential to improve performance with the adjustable propeller and engine that will produce matching so that high efficiency will be obtained. Well designed propellers can generally achieve 80% efficiency in their best operating areas. [1]

One of the UAV prototypes produced by LAPAN is LSU-03. That UAV uses pusher type of propeller. The existing propeller is made of wood. One of the weaknesses of wood is not withstand the age and the unfavorable mechanical properties. To improve structural strength and better mechanical properties, the propeller will then be made using composite materials. Before designing the composite material, aerodynamic load distribution is calculated along the surface of the propeller blades.



This research aims to obtain aerodynamic load distribution along the surface of the propeller blades. The aerodynamic load distribution is expected to be used as input in designing the composite structure of the propeller blades.

The aircraft propeller that will be simulated and analyzed for their structural strength are the LSU-03 (LAPAN Surveillance UAV - 03) propeller. The aircraft is designed as a high-performance unmanned aircraft for mapping and surveying in small to medium areas. This aircraft can fly for 4 hours with a load of 5 kg with a cruise speed of 80 km / h and a maximum speed of 110 km/h with a flying height cruise 1000-2000 m. The power used is a piston engine with a capacity of 60 cc and power output of 6 hp @ 8000 rpm using fuel octane 92. Engine power is connected through the shaft to the propeller 2 blades with the size 24 x 10 pusher type. [2]



Figure 1. LSU-03 Aircraft [2]

2. Methodology

In this research, the method to calculate analytical aerodynamic load is using the blade element theory. The Blade Element Theory (BET) is a relatively simple model to predict the performance of a certain propeller geometry. In BET the propeller blade is subdivided in small elements and the two-dimensional flow around each element is analyzed individually. [3]

The BET is assumed that the behavior of an element is not affected by adjacent elements of the same blade, the airfoil characteristic is adopted for the element, and the effective velocity of the element by air is the resultant axial velocity, rotation speed and velocity imposed. [4]

The theory of aircraft propellers, following the original development of finite wing theory, has nearly always proceeded as a lifting line analysis. That is, blade elements may be considered to act as two-dimensional foils upon which the forces are the same as would be found in a uniform two-dimensional flow with the same velocity and direction as occurs locally at the blade element. This approach to the design of blade elements is continued in the present study. [5]

Data on blade elements theory are airfoil geometry of each segment, chord length, twist angle, lift coefficient, drag coefficient and rotary speed propeller.

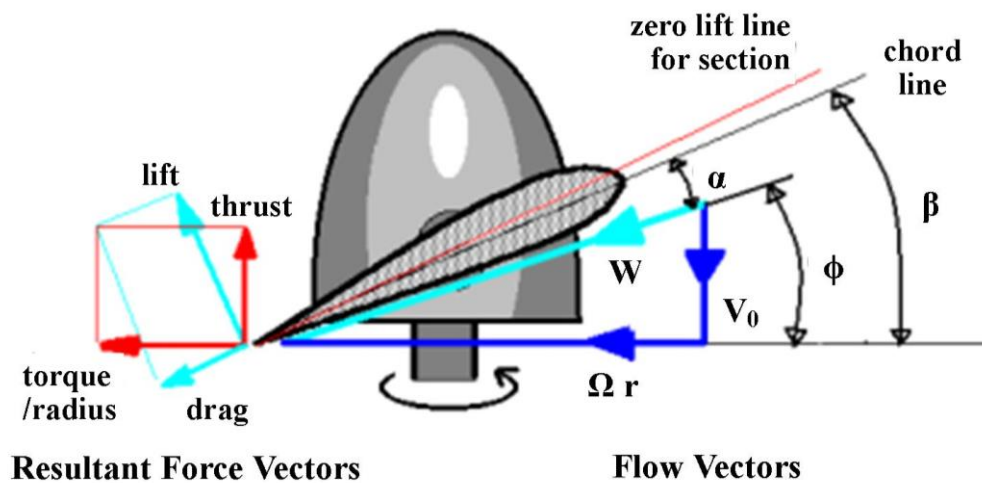


Figure 2. Classic blade element theory [4]

The formula of blade element theory:

$$l = \frac{1}{2} \rho W^2 c C_l \quad (1)$$

$$d = \frac{1}{2} \rho W^2 c C_d \quad (2)$$

$$C_l, C_d = f(\alpha) \quad (3)$$

$$W = \sqrt{V_0^2 + (\Omega r)^2} \quad (4)$$

$$T = B(l \cos \phi - d \sin \phi) \quad (5)$$

where l is lift, d is drag, W is resultant velocity, ρ is air density, c is chord, C_l is lift coefficient, C_d is coefficient drag, V_0 is axial velocity, Ωr is tangential velocity, B is the number of propeller blades, ϕ is angle of velocity and T is thrust.

The propeller is rotated at a speed of 7000 RPM with axial velocity (flight speed) of 20 m/s, this condition is equal to the condition at the time of take-off aircraft which the propeller receives the maximum load. The propeller having two blades has a hub diameter of 0.052 m and a tip diameter of 0.6 m. ρ is 1,225 kg/m³.



Figure 3. Original propeller (a), 3-D CAD propeller model (b)

The propeller model LSU-03 by modeling the specification of an existing propeller using 3D scan and converted in Computer Aided Design(CAD) with Solidworks parametric for easy change in geometry.

Aerodynamic load calculations were performed using CFD 3-D simulation method with Ansys software with CFD CFX which is included in this software. Prior to entering the simulation stage, a 3-D CAD plane model was made using Solidworks software as an input geometry model for simulation.

The CFD simulation reliability depends on many aspects, including computational domain sizing, mesh size and quality as well chosen solution type (steady state or transient) and physical formulation (type of equation solved, additional wall formulations and corrections) [6].

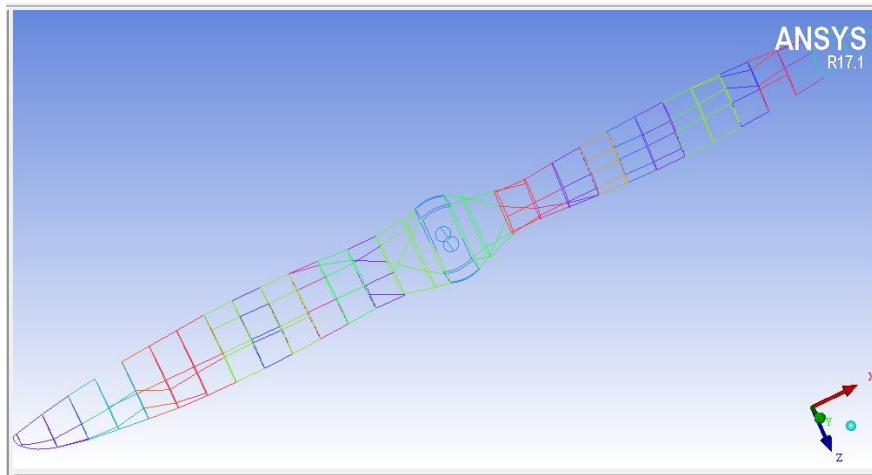


Figure 4. 3-D CAD propeller model has been converted to Ansys

The simulation stages to obtain aerodynamic load on the propeller are as follows: first make a 3-D CAD model of the propeller. In Figure 4 show of CAD model geometry from solidworks to ansys to create fluid flow domains and their boundaries.

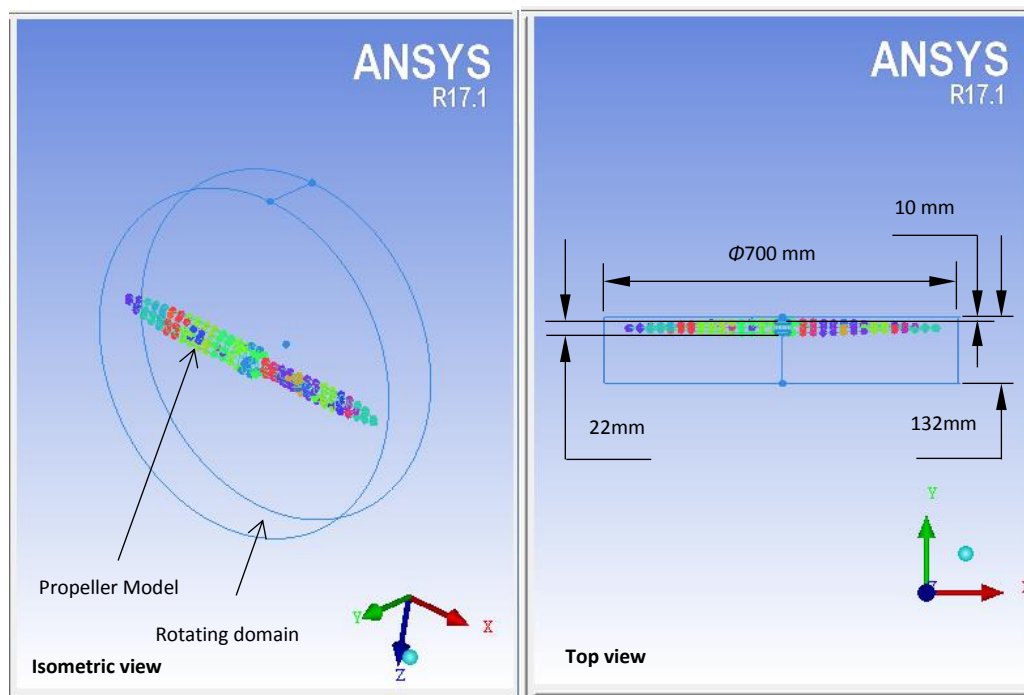


Figure 5. Rotating domain

By using the ICEM software (part of Ansys) 3-D geometry model is imported for the creation of rotating domain with space interfaces for cylindrical rotation space of 0.7 m diameter with a distance of 10 mm from the surface of the front propeller and 100 mm from the surface of the rear propeller (see figure 5). For the cylindrical field (static domain) has a dimension of 10 m diameter with a cylinder length of 10 m and the distance from the front side of the static space to the front of the rotation space of 1.5 m (see figure 6).

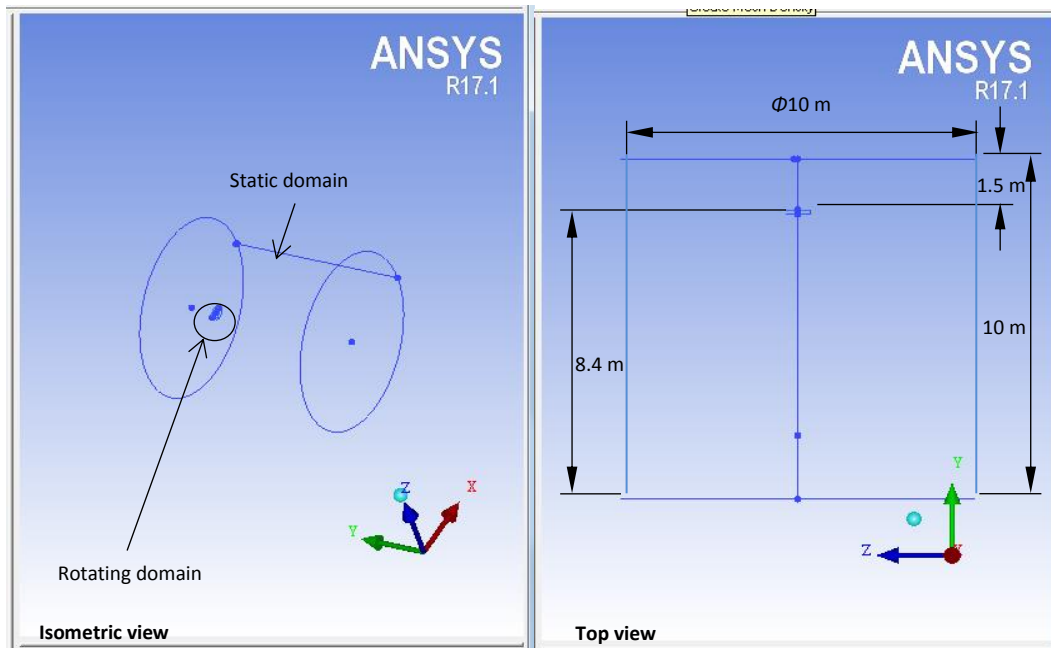


Figure 6. Static domain

After that created the input, output to define fluid flow limits for each surface. Do the meshing process, with tetra/mixed mesh type and robust mesh (octree) mesh method, this meshing applied to rotation domain and static domain. The rotating mesh composition has a size of 1.25 for the propeller, 14 for the front (input) and rear (output) and 7 for the tube. And static mesh made with size 14 for the front (input), rear (output) and tube. In static mesh arranged in more detail by using the ratio at 1.4 so the denser of mesh more dense in the middle.

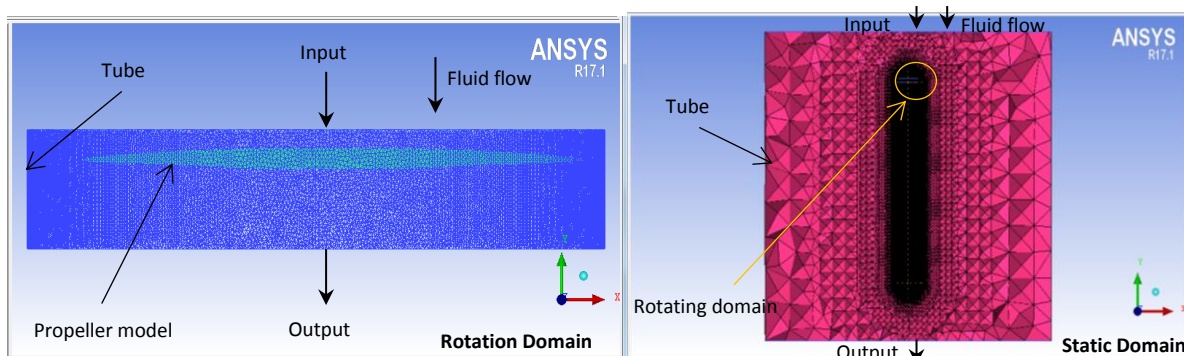


Figure 7. Meshing results

After meshing, open CFX-Pre is still part of Ansys software to enter the boundary conditions of fluid flow.

The rotation domain are set for Basic Setting and Fluid Model as follows: The rotation domain of Basic Setting are for material: “*Air Ideal Gas*”, domain option: “*Rotating*”, angular velocity: “*7000 [rev min⁻¹]*” and rotation axis: “*Global Y*”. And Fluid Models are for heat transfer option: “*Total Energy*” and turbulence option: “*Shear Stress Transport*”.

On the static domain consist of opening, inlet and outlet side are set as follows:

1. Opening side (tube) setting, set the Basic Setting on Boundary Type: “*Opening*”. The Boundary Details on Mass and Momentum Option: “*Cart Vel Components*” at $V = 20 [m s^{-1}]$ and Opening Temp.: at “*25°C*”.
2. Inlet side setting, set the Basic Setting on Boundary Type is “*Inlet*”. The Boundary Details on Flow Regime Option: “*Subsonic*”, Mass and Momentum Option: “*Normal Speed*”, Normal Speed: $20 [m s^{-1}]$; and Static Frame Total Temp.: “*25°C*”.
3. Outlet side setting, as follows set the Basic Setting on Boundary Type is “*Outlet*”. The Boundary Details on Flow Regime Option: “*Subsonic*”, Mass and Momentum Option: “*Static Pressure*” and Relative Pressure: “*0 (Pa)*”.

The simulation is carried out at the condition of the flight speed of 20 km/h and the rotational speed of 7,000 rpm. The CFD 3-D simulation results will be validated using Blade Element Theory.

From the propeller geometry, a 3-D rotational aerodynamic model (CFD CFX) is applied to obtain the pressure / load distribution on the propeller. The CFD result of the pressure distribution is compared with the analytical calculation result using the Blade Element Theory (BET) method. After CFD simulation, for the next research use the Direct Import CFD (One-Way Fluid Structure Interaction) method then mapping to match the CFD model with Finite Element Method (FEM) in Ansys software.

3. Result and Analysis

a) Analytical Result

The data of C_l and C_d based on the angle of attack (α) were obtained using CFD 2-D by incorporating the airfoil geometry of the propeller and its condition, as shown in Table 1 and Figure 8 below.

Table 1. Data of lift coefficient and drag coefficient

Angle of Attack α	Lift Coefficient C_l	Drag Coefficient C_d	L/D
-10	-0.344	0.023	-15.088
-9	-0.279	0.021	-13.037
-8	-0.214	0.020	-10.700
-7	-0.142	0.019	-7.358
-6	-0.070	0.019	-3.763
-5	0.006	0.018	0.302
-4	0.081	0.018	4.481
-3	0.153	0.018	8.453
-2	0.221	0.046	4.846
-1	0.291	0.050	5.879
0	0.374	0.051	7.305
1	0.432	0.020	21.818
2	0.497	0.021	24.010
3	0.559	0.022	25.760
4	0.617	0.023	26.826
5	0.671	0.025	27.388

6	0.723	0.026	27.490
7	0.772	0.029	27.088
8	0.817	0.031	26.355
9	0.817	0.031	26.355
10	0.817	0.031	26.355

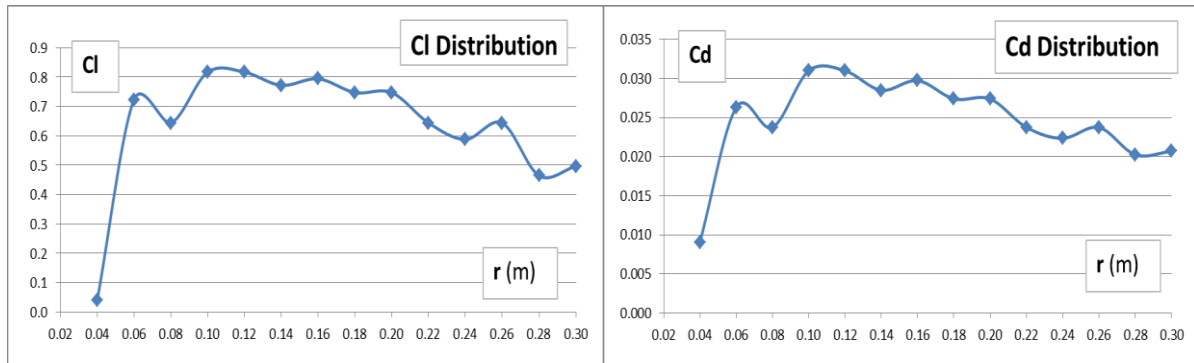


Figure 8. Graph of lift coefficient C_l and drag coefficient C_d distribution

Figure 8 shows that the value of C_l along the blade ranges from 0.5 to 0.8. The value of C_l at the root is get near to zero because its section is not airfoil. C_l value tend to decrease from the position of root to tip because the angle of attack which also decreases. Similarly, with the value of C_d because the value of C_l and C_d is a function of angle of attack.

The value of lift and drag are obtained from equations (1) and (2). Chord and twist angle distributions are presented in Table 2 as below.

Table 2. Chord and twist angle distributions

Segment	Radius, r (m)	Chord, c (m)	Twist Angle, β (deg)
1	0.04	0.0413	29.36
2	0.06	0.0414	30.40
3	0.08	0.0440	23.34
4	0.10	0.0455	23.18
5	0.12	0.0469	21.20
6	0.14	0.0472	18.20
7	0.16	0.0470	17.00
8	0.18	0.0456	15.00
9	0.20	0.0435	14.30
10	0.22	0.0403	11.35
11	0.24	0.0360	10.00
12	0.26	0.0310	10.70
13	0.28	0.0236	7.00
14	0.30	0.0080	8.00

Table 2 shows the chord distribution tends to decrease from root to tip. It is intended that the aerodynamic load at the tip of the blade is not too large. The table also shows that the twist angle distribution also decreases from root to tip. It is also intended that the aerodynamic load at the tip of

the blade is not too large. The twist angle at the root is made larger to increase the strength of the structure in that area.

The speed distribution is calculated using equation (4). The results are presented in Figure 9 as below.

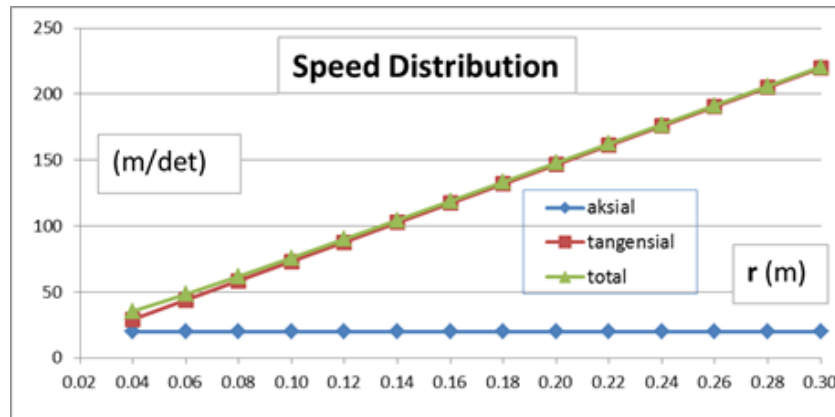


Figure 9. Graph of speed distribution

The axial velocity distribution in Figure 9 has constant value. Because of the assumption used is not difference in angle between the axial position of the propeller with the flight direction of the plane. The tangential velocity has enlarged to the tip and the value r increasingly large. By summing up the constantly axial velocity with the enlarged of tangential velocity at the tip of the blade, the enlarged of total velocity is obtained.

After all the necessary parameters have been fulfilled, we get the value of lift and drag in each segment of the blade. The distribution of lift and drags is shown in Figure 10.

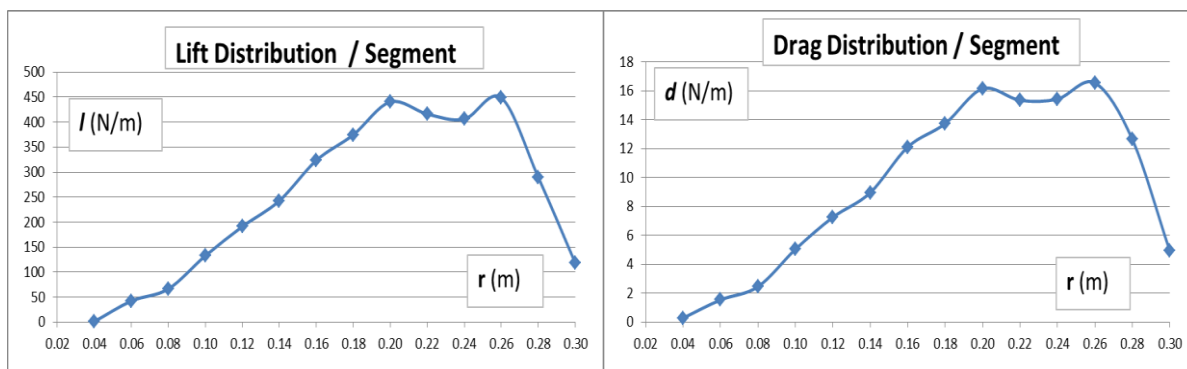


Figure 10. Graph of lift and drag distribution

Figure 10 shows that the value of lift and drags is getting increase at the tip of the blade. That caused the value of the total speed is getting bigger in that area.

The amount of thrust in each segment is calculated by equation (5). The distribution of the calculation results is presented in Figure 11 as below.

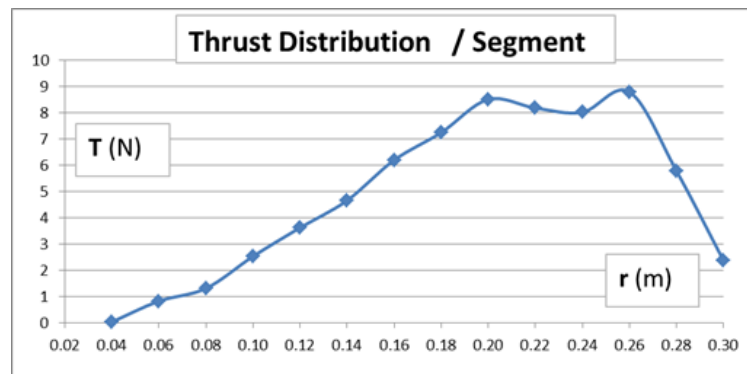


Figure 11. Graph of thrust distribution

Figure 11 above shows that the thrust is getting larger in the tip area of the blade. That caused the lift is getting bigger in that area.

The calculation results using analytical aerodynamic load calculation obtained a thrust for each blade of 68 N and the total thrust force of the propeller is 136 N.

b) CFD Result

After all is done, then the next step is done running to get the simulation results. Two simulations were performed, for the second simulation, the addition of mesh on the surface of the propeller with the prism mesh so that the boundary layer on the surface of the propeller can be analyzed in more detail.

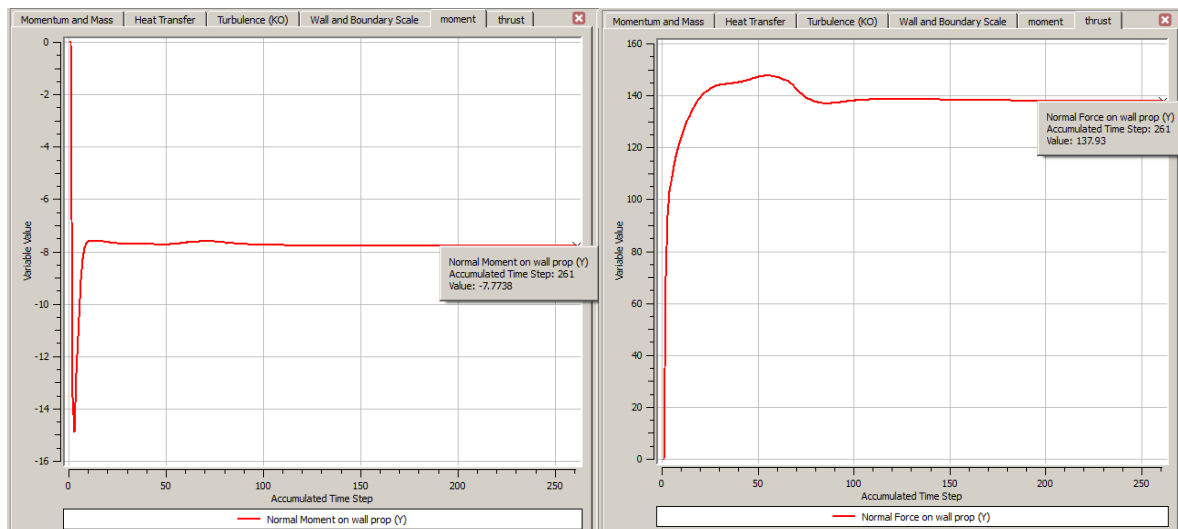


Figure 12. Graph of blade moment and thrust to number of iterations for CFD simulation type 1 (without prism mesh)

From figure 12 and 13 show graph the moment and thrust on the propeller has not changed even though the iteration process is reproduced. The addition of iteration will not have much effect on the results obtained. For CFD simulation type 1 and 2, the moment and thrust obtained not too far.

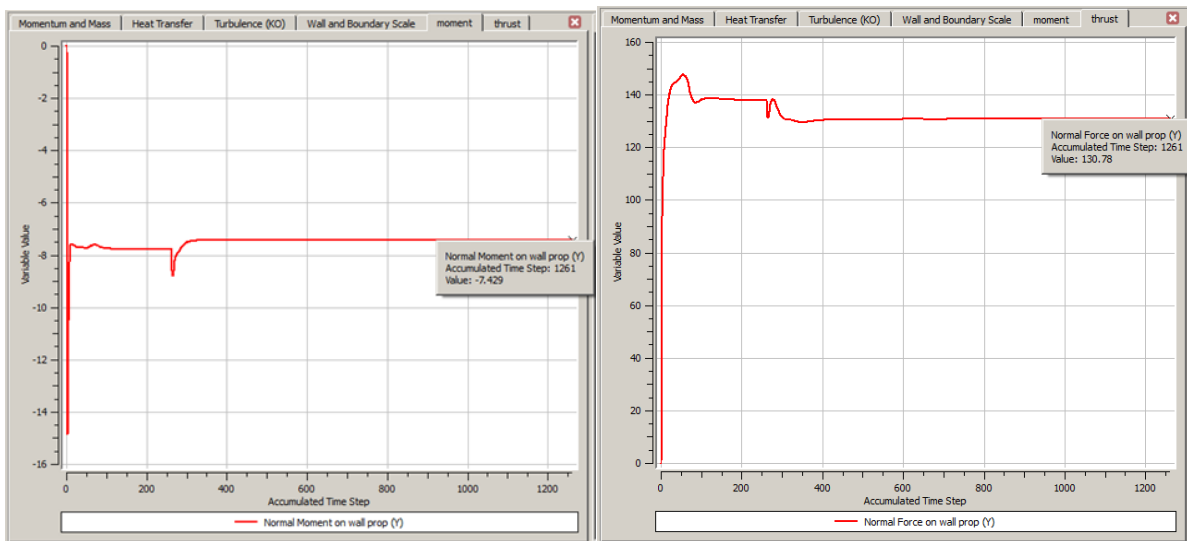


Figure 13. Graph of blade moment and thrust to number of iterations for CFD simulation type 2 (with prism mesh)

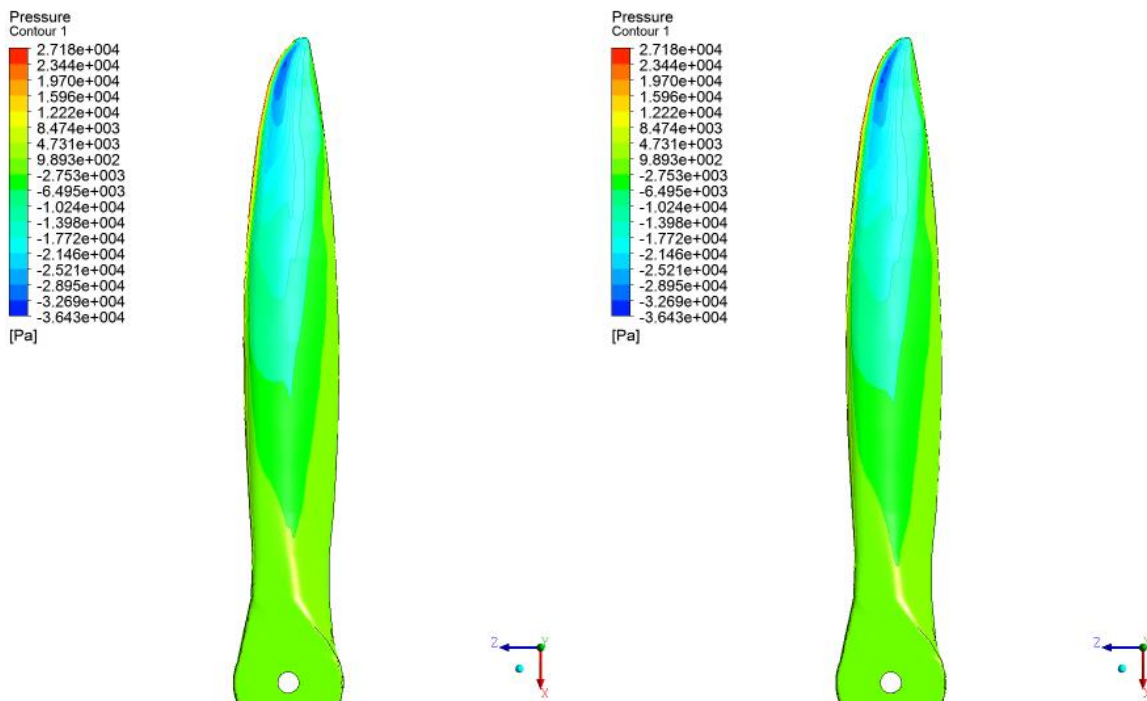


Figure 14. The pressure distribution on the front of the blades, without prism mesh (right) with prism mesh (left)

From the figures 14 and 15 it appears that the result of the pressure distribution is not very different between the simulations using prism mesh and without prism mesh.

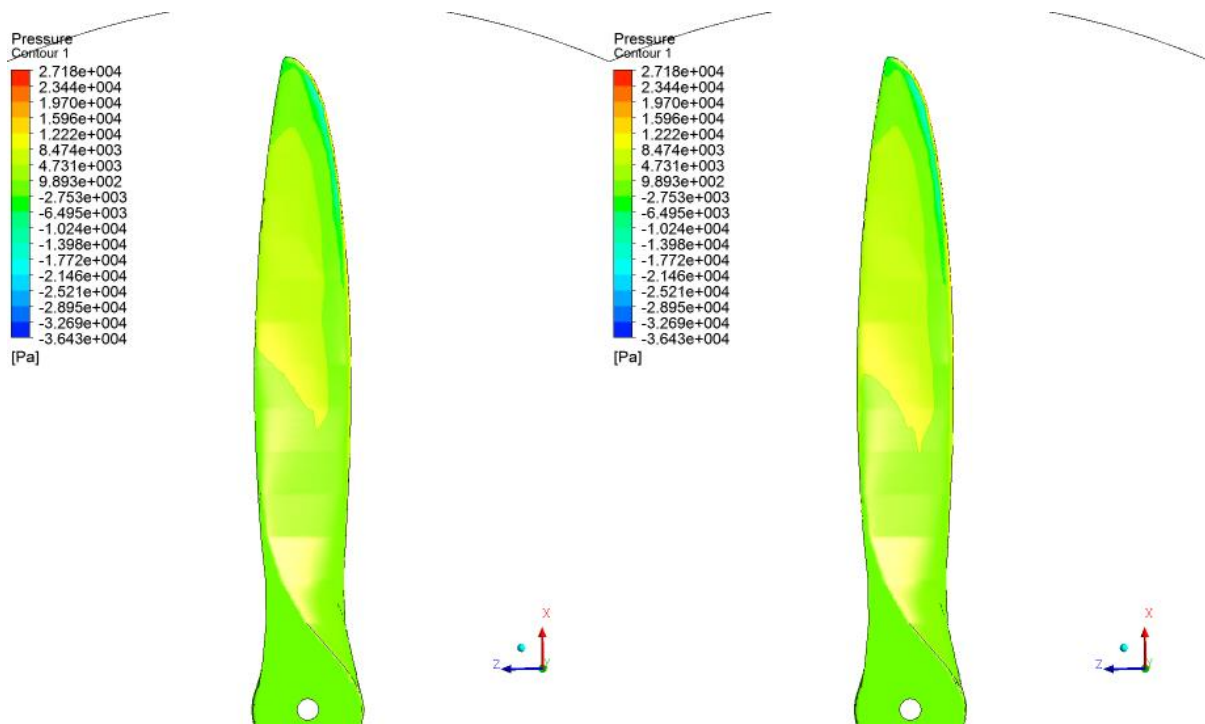


Figure 15. The pressure distribution on the rear of the blades, without prism mesh (right) withprism mesh (left)

Table 3. Result of CFD simulation

	CFDsimulation(Type 1)	CFDsimulation (Type 2) (with prism mesh)
<i>Thrust (Newton)</i>	137.7	130.5
<i>Power (Watt)</i>	5844	5601
<i>Effisiensi (%)</i>	47.1	46.6

Obtained by analytic and numerical calculation of aerodynamic load as follows:

Table 4.Comparison of analytic and numerical calculations

	Analytic	CFD simulation (Type 1)	CFD simulation (Type 2) (with prism mesh)
<i>Thrust (Newton)</i>	136	137.7	130.5
Percentage of Analytic vs CFD (%)		1.2	4.1
Percentage of CFDTyep 1 vs Type 2 (%)		5.2	5.2

From other paper references obtained, CFD analysis the thrust and torque for our propeller are 1007N and 311.19Nm which are 22.3% and 21.3% less than the theoretical calculated values. [7]The percentage of analytic and CFD calculation in this research is smaller than reference data so the comparison is acceptable.

4. Conclusions

From the analytic and numerical simulation results of aerodynamic load of propeller, the conclusion are: blade element theory useful for quick calculation at conceptual design stage. It gives lift and drag coefficient at various position of the propeller.

Numerical calculation based on prismatic mesh will provide more accurate pressure distribution along the propeller span. Two mesh type gives 1.2 % difference for type 1 and 4.1% for type 2 compared to blade element theory result. Both approaches could be used for structural design stage.

Acknowledgment

I would like to thank Faculty of Mechanical Aerospace Engineering ITB and National Institute of Aeronautics and Space (LAPAN) for supporting this research.

Reference

- [1] allstar. Propeller Aircraft Performance and The Bootstrap Approach. [Online] Allstar Network, January 18, 2011. <http://www.allstar.fiu.edu/aero/BA-Background.htm>.
- [2] LSU-03 Datasheet, LSU-03 UAV Platform, Pusat Teknologi Penerbangan, LAPAN, 2015.
- [3] Mario Heene, Aerodynamic Propeller Model for Load Analysis, Master of Science Thesis, Royal Institute of Technology School of Engineering Sciences, Stockholm Sweden 2012.
- [4] F. Hartono, Metode Perancangan dan Analisis Low Reynolds Number Propeller, Aerospace Indonesia Meeting 2005.
- [5] Q.R. Wald. The aerodynamics of propellers. *Progress in Aerospace Sciences*, 2006.
- [6] Mateusz Stajuda, Maciej Karczewski, Damian Obidowski, Krzysztof Jozwik, Development of a CFD model for propeller simulation, *Lodz University of Technology Institute of Turbomachinery*, Vol. 20, No. 4 (2016) 579–593
- [7] Arif Ahmed Sohel, Md., Abdus Shamir Talukder & Dr. Mohammad Arif Hasan Mamun, Constant Pitch Propeller Design for Low Subsonic Airplane, *Global Journal of Researches in Engineering: A Mechanical and Mechanics Engineering*, Volume 14 Issue 6 Version 1.0 Year 2014